THE JOURNAL OF PHYSICAL CHEMISTRY B

ARTICLE

pubs.acs.org/JPCB

Hydrogen Bonding Behaviors of Binary Systems Containing the Ionic Liquid 1-Butyl-3-methylimidazolium Trifluoroacetate and Water/Methanol

Qing-Guo Zhang,[†,‡] Nan-Nan Wang,[†] Shuang-Long Wang,[‡] and Zhi-Wu Yu*[,†]

[†]Key Laboratory of Bioorganic Phosphorous Chemistry and Chemical Biology (Ministry of Education), Department of Chemistry, Tsinghua University, Beijing 100084, P. R. China

[‡]Department of Chemistry, Bohai University, Jinzhou 121000, P. R. China

Supporting Information

ABSTRACT: The hydrogen-bonding properties of binary systems consisting of a representative Brønsted acidic hydrophilic ionic liquid (IL) 1-butyl-3-methylimidazolium trifluoroacetate ([Bmim][CF_3CO_2]) and a cosolvent, water or methanol, over the entire concentration range have been investigated by methods of attenuated total reflectance infrared spectroscopy, ^{1}H NMR spectroscopy, and quantum chemical calculations. It has been found that the hydrogen-bonding interactions between the anion [CF_3CO_2]$^-$, rather than the cation, and the cosolvent molecules are dominant at low concentration of cosolvent. The H-bond interaction site between the IL anion and water/methanol is the O atom in the −COO group, while the −CF_3 group makes a positive contribution by donating electron to the carboxylic group, forming a cooperative hydrogen-bonding system. For the cation [Bmim]$^+$, although the C2−H is the favorable proton donor in H-bonding interactions, the water/methanol molecules form H-bonds with the alkyl C−H at low water/methanol concentration due to the stronger interaction between C2−H and [CF_3CO_2]$^-$. Interestingly, we found that the interaction between methanol and the IL is stronger than that between water and the IL because the methyl group in methanol has a positive contribution to the formation of H-bonds. The following sequential order of interaction strength is established: [Bmim]$^+$−methanol−[CF_3CO_2]$^-$ > [Bmim]$^+$−water−[CF_3CO_2]$^-$ > [Bmim]$^+$−[CF_3CO_2]$^-$ > [CF_3CO_2]$^-$−methanol > [CF_3CO_2]$^-$−water > [Bmim]$^+$−methanol > [Bmim]$^+$−water.

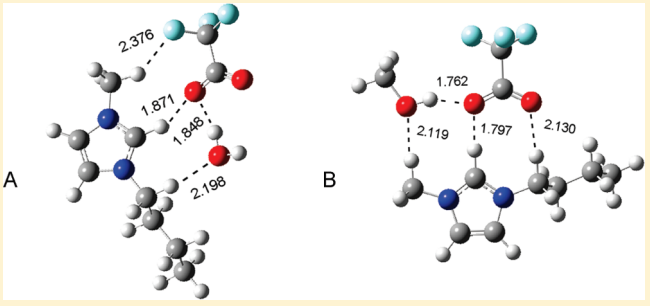

1. INTRODUCTION

Ionic liquids (ILs) are attracting more and more attention from both academic and industrial communities because of their unique properties as a potential green solvent and reaction medium.[1−17] A very special property of ILs is that they can be tailored by selecting the required anions and cations with specific properties. Ionic liquids, therefore, are also called "designer solvents"[18−20] and can fulfill a wide range of specific needs. Despite tremendous efforts devoted to ILs in recent years, they are still not easily available and are expensive for practical applications. Then, how to design ILs with super properties and of cheaper and easier preparation has become an urgent issue for the applications of ILs. This requires a deeper understanding of the physical properties of ILs, including the structure−property relationship and interaction patterns between ILs and other molecules.

As is known, many hydrophilic ILs are hygroscopic and are actually entirely miscible with water or polar organic liquid substances.[21−24] It has been a common practice that IL + cosolvent mixtures are used as working fluids in application processes in fields like catalysis, synthesis of new materials, separation, and electrochemistry.[25−30] Efforts focusing on the properties of various forms of mixed IL + cosolvent systems, particularly when water is used as the partner, have been made by a number of research groups in recent years.[12−16,31−43] To better develop practical IL + cosolvent systems for various purposes, it is necessary to examine in detail the interactions between ILs and solvents, especially the hydrogen-bonding behaviors of the systems of interest.

Generally speaking, hydrogen bonds are believed to play an important role in the interaction between ILs and cosolvents. Some experimental and theoretical investigations concerning H-bonding interactions have been carried out to understand the property and structural changes of ILs induced by cosolvents.[33−39,44−55] Ludwig's group reported that water in ILs could be a more reliable measure of the dielectric constant and polarity of ILs.[44] Cammarata et al. found that water molecules absorbed by imidazolium-based ILs from air (0.2−1.0 mol dm^{-3})

Received: May 9, 2011
Revised: August 12, 2011
Published: August 16, 2011

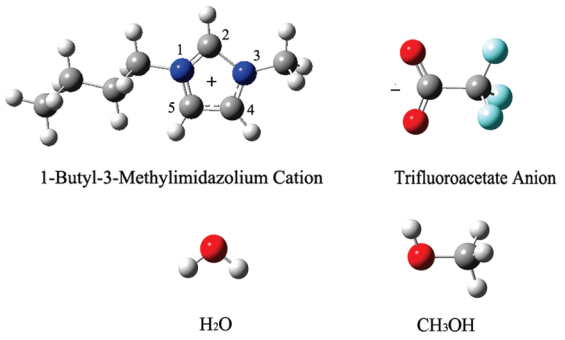

Figure 1. Chemical structure and atom numbering for 1-butyl-3-methylimidazolium trifluoroacetate ([Bmim][CF_3CO_2]), H_2O, and CH_3OH.

mainly interact with the anions and exist in symmetric anion−HOH−anion H-bonded complexes as revealed by infrared spectroscopy. Various anions were selected to compose the ILs, and a sequential order of H-bonding strength between water and different anions was suggested.[45] Porter and co-workers proposed that, even at low water content, $2H_2O$−anion H-bonded complexes could also exist.[46] The sequential addition of water to pure ILs gradually destroys the three-dimensional network structure of ILs, first into ionic clusters, then into ionic pairs surrounded by water molecules, and ultimately into fully hydrated separated ions.[47,48] Takamuku et al. found that the state of water molecules in 1-ethyl-3-methylimidazolium tetrafluoroborate ($EMIBF_4$) changes markedly at $x_w \approx 0.3$.[49] There have also been reports on the H-bonding interactions in the mixtures of ILs and other cosolvents such as dimethyl sulfoxide and methanol. For example, Li's group found that the H-bond between the S═O group of DMSO and the IL cation contributed significantly to the blue-shifted C−D stretching vibrations of DMSO-d_6.[36] These results indicate that anions of ILs are usually the primary factor of the interaction between ILs and water or other cosolvents. Thus it is of importance to carry out more investigations on the H-bonding interactions concerning ILs with different anions, especially those ILs with hygroscopic background, as they are common, low in cost, and easily available.

Recently, we studied the H-bonding interactions in binary systems of 1-ethyl-3-methylimidazolium ethyl sulfate (EMIES) + water[38] and 1-butylpyridinium tetrafluoroborate ($BuPyBF_4$) + water/dimethyl sulfoxide.[39] The similarity and difference on interaction sites and sequences of H-bonding interaction strength between ILs and water/DMSO were discussed. As a continuous work, we selected a representative Brønsted acidic ionic liquid 1-butyl-3-methylimidazolium trifluoroacetate ([Bmim][CF_3CO_2]), which is believed to have great industrial potential,[56,57] to investigate the hydrogen-bonding behaviors when it is mixed with cosolvents. This IL has an anion with a favorable proton-accepting site −COO (see Figure 1) and may show interesting H-bonding interaction behaviors. To our knowledge, there have been few publications concerning the hydrogen-bonding interaction of [Bmim][CF_3CO_2].[45,58] Cammarata et al. studied the strong interactions between −COO and water absorbed from air and suggested that the anions could be a precursor of the water miscibility with trifluoroacetate-based ionic liquids.[45] In an earlier work, Bonhote et al. determined the viscosities of the IL and proposed that they are governed by van der Waals interactions and H-bonding.[58]

The selected cosolvents to interact with this hydrophilic IL in this work are water and the common protonic solvent CH_3OH. Compared with H_2O, CH_3OH is of lower polarity and can be considered as a derivative of HOH, when an H atom is replaced by a hydrophobic methyl group. The two cosolvents are supposed to show some differences in the H-bonding interactions.

Among various experimental techniques, infrared spectroscopy is a powerful and convenient approach to study the H-bonding interactions at the molecular level.[38−45,59−64] Herein, we have investigated the hydrogen-bonding behaviors of [Bmim][CF_3CO_2]−water and [Bmim][CF_3CO_2]−methanol binary systems over the entire concentration range using attenuated total reflectance infrared spectroscopy (ATR-IR), ^{1}H NMR spectroscopy, and density functional theory (DFT) calculations. In particular, excess infrared absorption spectroscopy,[38,39,60−64] which is developed in our laboratory and can enhance spectral resolution in liquid solutions,[60−64] has been employed to reveal details of the molecular interactions.

2. EXPERIMENTAL SECTION

2.1. Chemicals. [Bmim][CF_3CO_2] was synthesized according to the literature.[54,61] The obtained product is a slightly yellow transparent viscous liquid. The chemical structure of [Bmim][CF_3CO_2] is described in Figure 1. The ^{1}H NMR chemical shifts of [Bmim][CF_3CO_2] are the following: δ_H (300 MHz, no solvent) 9.34(C(2)H); 7.69(C(4)H); 7.61(C(5)H); 4.05(NCH_2); 3.78(NCH_3); 1.57($NCCH_2$); 1.02($NCCCH_2$); 0.60($NCCCCH_3$). These data are in good agreement with literature values.[58,65] Water content after drying, measured by Karl Fisher titration, is 1.3×10^{-3} mass fraction. Deionized water was further distilled in a quartz still, and the conductivity is $(0.9-1.3) \times 10^{-4}$ S·m^{-1}. D_2O and CD_3OD were purchased from Aldrich (99.9 D%).

2.2. Sample Preparation. A series of [Bmim][CF_3CO_2]−D_2O and [Bmim][CF_3CO_2]−CD_3OD binary mixtures were prepared by weighing. The mole fractions of D_2O in [Bmim][CF_3CO_2]−D_2O mixtures are 0.0987, 0.2018, 0.2993, 0.4006, 0.4993, 0.6019, 0.7024, 0.7968, and 0.8970. The mole fractions of CD_3OD in [Bmim][CF_3CO_2]−CD_3OD mixtures are 0.0916, 0.1885, 0.2947, 0.3762, 0.4806, 0.5746, 0.6720, 0.7858, and 0.8984.

2.3. FTIR Spectroscopy. FTIR spectra over the range from 4000 to 650 cm^{-1} were collected at room temperature (~25 °C) using a Nicolet 5700 FTIR spectrometer, equipped with a DTGS detector. Two attenuated total reflection (ATR) cells were employed in the experiments. They are made of trapezoidal ZnSe/Ge crystals with incident angles of 45°/60° and 12/7 reflections. The Ge crystal, with fewer numbers of reflections and thus shorter effective light path, was used to examine the strong stretching bands of −CO and $-CF_3$. Spectra were recorded with a resolution of 2 cm^{-1}, a zero filling factor of 2, and 16 parallel scans. For each sample, three parallel measurements were carried out. The refractive indexes of solutions were measured with a refractometer at 25 °C. The formulas suggested by Hansen[66] were used to do the ATR corrections.

2.4. Excess Absorption Spectroscopy. The theory of excess absorption spectroscopy has been described in detail elsewhere.[62,63] Briefly, an excess infrared absorption spectrum is defined as the difference between the spectrum of a real solution and that of the respective ideal solution under identical conditions. The working equation in calculating the excess infrared

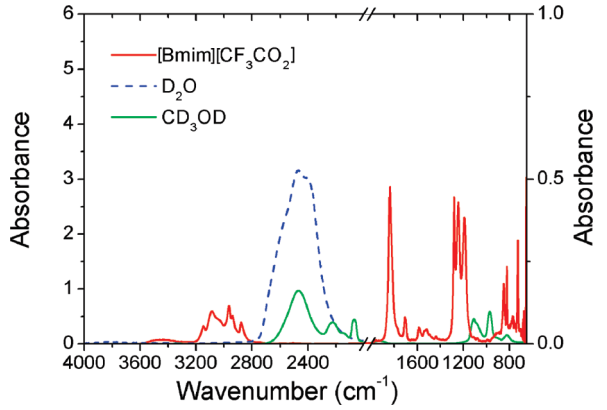

Figure 2. ATR-IR spectra of $[Bmim][CF_3CO_2]$, D_2O, and CD_3OD determined with ZnSe (in the range of 4000−1900 cm^{-1}, left absorbance axis) and Ge (in the range of 1850−680 cm^{-1}, right absorbance axis) ATR crystals.

absorption spectrum is

$$\varepsilon^{E} = \frac{A}{d(C_1 + C_2)} - (x_1\varepsilon_1^* + x_2\varepsilon_2^*) \quad (1)$$

where A is the absorbance of the mixture, d is the light path length, C_1 and C_2 are molarities of the two components, x_1 and x_2 are mole fractions of components 1 and 2, and ε_1^* and ε_2^* are molar absorption coefficients of the two components in their pure states, respectively.

The calculation of the excess infrared spectra was programmed using Matlab 7.0 (Math Works Inc., Natick, MA). The data manipulations, i.e., the subtraction, truncation, and baseline correction of the IR spectra, were also performed using Matlab 7.0.

2.5. ^{1}H NMR Measurements. The ^{1}H NMR spectra of samples were obtained on a JEOL JNM-ECA 300 NMR spectrometer at 298 K with TMS as internal standard.

2.6. Quantum Chemical Calculations. The geometries, binding energies, harmonic vibrational frequencies, and IR intensities were obtained by density functional theory (DFT) at the 6-31++G(d,p) basis set with the Gaussian 03 program.[67] DFT has been used extensively to study the interactions between ionic liquids and cosolvents such as water, acetone, and DMSO.[36−39,51,68−70] We selected the 6-31++G(d,p) basis set in our calculation following those studies. The optimized geometries were recognized as local minima with no imaginary frequency.

3. RESULTS AND DISCUSSION

3.1. ATR and Excess Infrared Spectra Analysis of Interactions between $[Bmim][CF_3CO_2]$ and Water. The partial ATR-FTIR of $[Bmim][CF_3CO_2]$ and D_2O are shown in Figure 2. The assignments of the stretching vibrations of the functional groups C−H, $-COO^-$, N−C═N, and $-CF_3$ in pure $[Bmim][CF_3CO_2]$ are assisted by the comparison between the observed and calculated frequencies of the respective vibration modes (Table 1). The scaling factor for the calculated frequencies is 0.955.[37,39] Absorption bands in the 3200−2800 cm^{-1} region are from C−H stretching vibrations, those above 3050 cm^{-1} are attributed to the imidazolium ring C−H stretches, while those below 3050 cm^{-1} are attributed to the alkyl C−H ($-NCH_3$ and $-NCH_2CH_2CH_2CH_3$) stretches.[71] For imidazolium ring

Table 1. DFT-Calculated and Observed Frequencies of the C−H, C═N, C═O, and $-CF_3$ Stretching Vibrations of the Main Groups in $[Bmim][CF_3CO_2]$

		frequency (cm^{-1}) (intensity)	
vibration	symbol	calcd[a]	obsvd
C4,5−H stretches	ν(C4,5−H)	3161(2)	3147
		3144(6)	
C2−H stretches	ν(C2−H)	2975(656)	3093
alkyl stretches	ν(alkyl C−H)	2972(35)	2965
		2962(35)	
		2941(19)	2938
		2929(18)	
		2922(38)	
		2898(38)	2878
		2889(25)	
		2885(10)	
$-COO^-$ stretches	ν($-COO^-$)	1637(481)	1686
N−C═N stretches	ν(N−C═N)	1518(135)	1574
$-CF_3$ stretches	ν($-CF_3$)	1148(331)	1200
		1113(249)	1169
		1071(285)	1123

[a] Calculated frequencies are scaled by 0.955. Data in parentheses are infrared intensities in km/mol.

C−H, the band at 3147 cm^{-1} is attributed to C4,5−H stretches and that at 3093 cm^{-1} is attributed to C2−H stretch.[51,72] The bands at 1686 and 1574 cm^{-1} are attributed to $-COO^-$ and N−C═N stretching vibrations, respectively, while the bands at 1200, 1169, and 1123 cm^{-1} are attributed to coupled $-CF_3$ stretching vibrations. These assignments are in agreement with literature work.[45]

ATR-IR spectra of binary mixtures of $[Bmim][CF_3CO_2]$−D_2O were recorded over the whole concentration range (mole fraction increment of about 0.1). D_2O was used to avoid the overlap of the O−H stretching vibration of water and the C−H stretching vibrations of the IL. The ATR-IR and excess infrared spectra of $[Bmim][CF_3CO_2]$−D_2O mixtures at different concentrations, including those of pure $[Bmim][CF_3CO_2]$ and D_2O, in the region of 3200−1050 cm^{-1} are shown in Figure 3. In the ATR-IR spectra (Figure 3A, B, C), the ν(C2−H), ν(C4,5−H), ν(O−D), and ν($-CF_3$) show blue shift, while the ν($-COO^-$) shows red shift upon addition of water. For ν($-CF_3$), only the band at 1123 cm^{-1} is analyzed because the other two bands at 1200 and 1169 cm^{-1} overlap with the bending vibration of D_2O (the very broad band shown in Figure 3C). The concentration dependences of the wavenumber shifts are summarized in Figure 5A. It should be noted that there is apparently an abrupt wavenumber shift of $-COO^-$ when x(water) is around 0.5. Reexamination of the respective IR band in Figure 3B finds that it actually consists of two overlapped peaks. Figure 3E further suggests that their positions are nearly fixed. The two peaks, therefore, are most likely from the $-COO^-$ in IL and in IL−water complex, respectively. And the apparent sudden shift in wavenumber happens at a concentration when the absorbance of the complex overpowers that of the ionic liquid.

According to the literature, the hydrogen bond involving aromatic C−H on the imidazolium ring is classified as red shift H-bond,[36,73] Thus the blue shifts of ν(C2−H) and ν(C4,5−H)

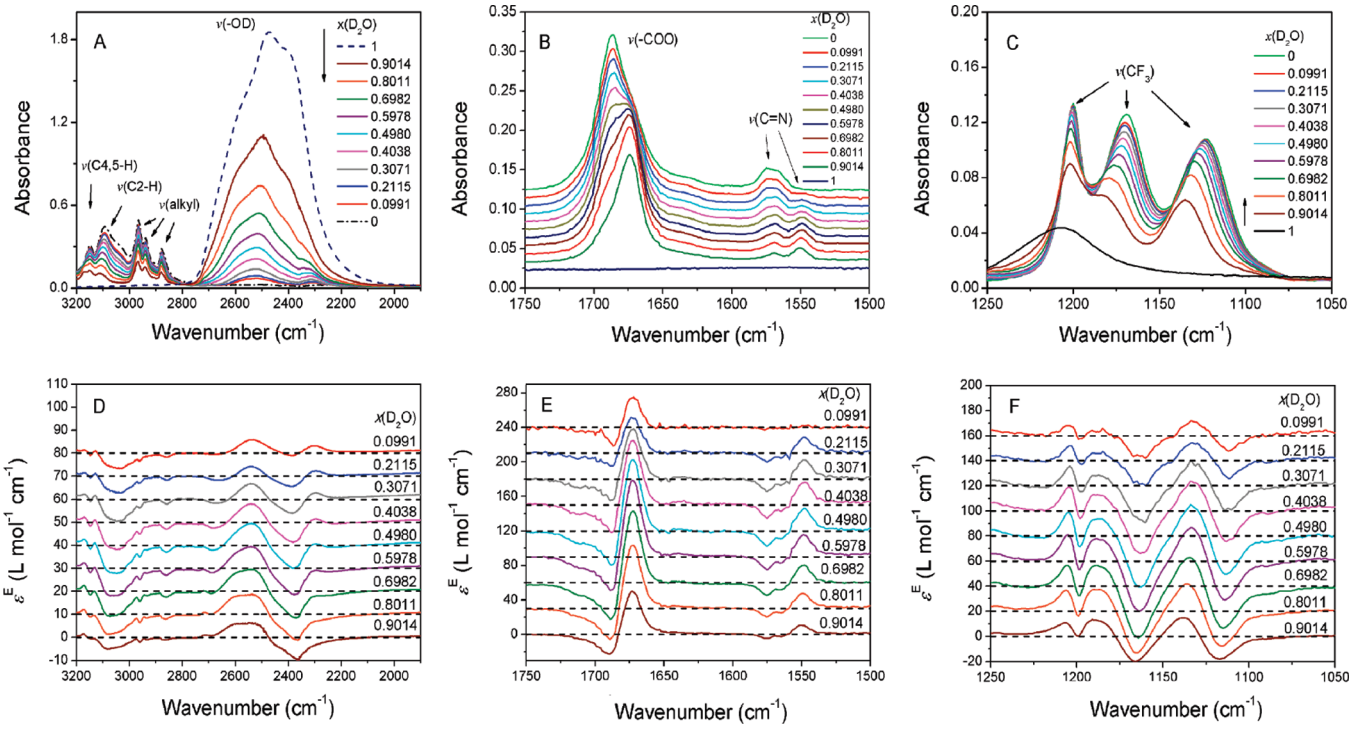

Figure 3. ATR-IR (upper) and excess infrared (lower) spectra of the $[Bmim][CF_3CO_2]-D_2O$ system in the range of the alkyl and −OD stretching vibration (A and D), the −COO and C═N stretching vibration (B and E), and the $-CF_3$ stretching vibration (C and F).

upon dilution observed in this work imply that water weakens the C−H···anion H-bonding interactions of $[Bmim][CF_3CO_2]$. Further, the blue shift of ν(C2−H) is about 13 cm^{-1} and that of ν(C4,5−H) is just 5 cm^{-1} (Figure 5A), indicating that the C2−H may have subjected to bigger influence upon dilution. This is in agreement with our understanding that C2−H is the most acidic hydrogen on the dialkylimidazolium cation[51] and the H-bond of C2−H···anion is stronger than that of C4,5−H···anion.[6] The H-bond involving O−D is also a red shift H-bond,[73] Thus, the blue shift feature of the O−D stretching vibration indicates that the H-bonds between D_2O and the cation/anion of $[Bmim][CF_3CO_2]$ are weaker than the cooperative H-bonds in pure water.

Excess infrared spectra can reveal the changes in molar absorptivity more clearly, providing information on the details of the molecular interactions in the mixtures and possible presence of new complexes. As can be seen in Figure 3D, the stretching vibrations of imidazolium ring C−H show positive bands at the higher wavenumber and negative bands at the lower wavenumber region. The positive ones are attributed to the new complexes involving C2−H and C4,5−H stretches, while the negative ones are from the complexes in pure ionic liquid. The stretching vibration of O−D also has a positive band around 2560 cm^{-1}, a negative band around 2360 cm^{-1} and a small positive band at ca. 2325 cm^{-1} (Figure 3D). The positive and negative bands around 2560 and 2360 cm^{-1} are attributed to the weaker D_2O−IL H-bond than the cooperative H-bonds in pure D_2O. The small positive band at ca. 2325 cm^{-1} which decreases with the dilution could be assigned to O−D stretching with one D_2O molecule interacting with two anions at low water concentration.

In Figure 3E, for $\nu(-COO^-)$ at about 1686 cm^{-1}, there is a negative band at the higher wavenumber and a positive band at the lower wavenumber, which are clear signals of the red shift of the absorption band. Since the red shift of $\nu(-COO^-)$ represents the weakening of C═O bond and the strengthening of the corresponding H-bond it participates in,[74] the results mean that the H-bond involving $-COO^-$ is enhanced in the dilution process. Considering the general understanding that $-COO^-$ is a good proton acceptor and, actually, a better proton acceptor than $-CF_3$,[45,75] we believe the dominant site of the H-bonding interaction between water and $[Bmim][CF_3CO_2]$ is $-COO^-$ of the anion. The theoretical results in a later section also support this conclusion.

For the vibration mode ν(N−C═N) at about 1574 cm^{-1}, there is a positive band at the lower wavenumber and negative bands at the higher wavenumber. The positive band at the lower wavenumber reflects the absorption of imidazolium ring in the new complexes when C2−H and C4,5−H form weaker H-bonds with water than in pure $[Bmim][CF_3CO_2]$.[38]

In Figure 3F, the excess spectra at around 1123 cm^{-1} have a positive band at the higher wavenumber and a negative band at the lower wavenumber, due to the blue shift of $\nu(-CF_3)$. Since the dominant interaction site between water and $[Bmim][CF_3CO_2]$ is $-COO^-$ of the anion, the blue shift of $\nu(-CF_3)$ is explained as the result of the cooperative move of the whole anion group, in which $-CF_3$ is an electron-donating group.[39,63] The electron-donating effect of $-CF_3$ in the formation of $[CF_3CO_2]^-\cdots H_2O$ H-bond will be confirmed by the theoretical calculation. The H-bonding behaviors in the $[Bmim][CF_3CO_2]-D_2O$ system discussed above suggest the possible existence of selective interactions among water and different functional groups of the cation and anion, while the preferable interaction group is the COO^- of anion.

3.2. ATR and Excess Infrared Spectra Analysis of the H-Bonding Interaction between $[Bmim][CF_3CO_2]$ and Methanol. Compared to the water molecule, the methanol molecule

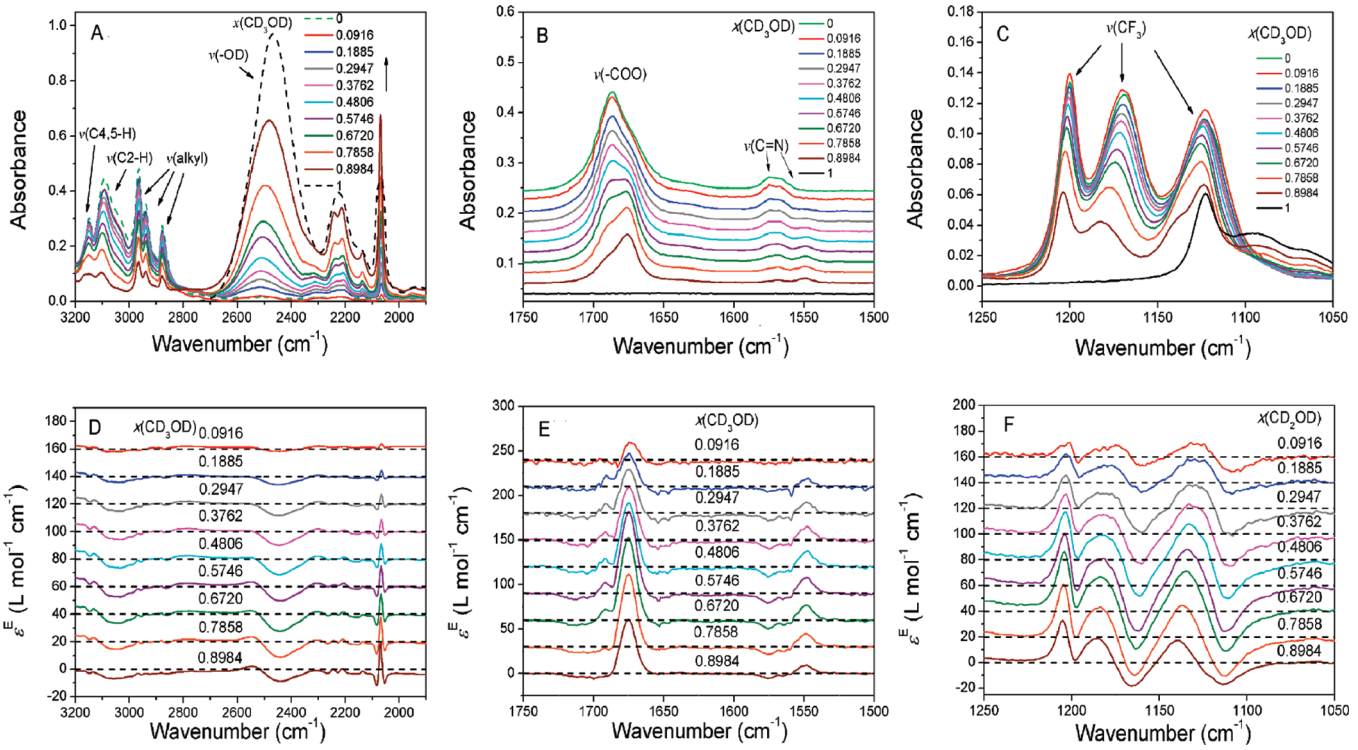

Figure 4. ATR-IR (upper) and excess infrared (lower) spectra of the $[Bmim][CF_3CO_2]-CD_3OD$ system in the range of the alkyl and −OD stretching vibration (A and D), the −COO and C═N stretching vibration (B and E), and the $-CF_3$ stretching vibration (C and F).

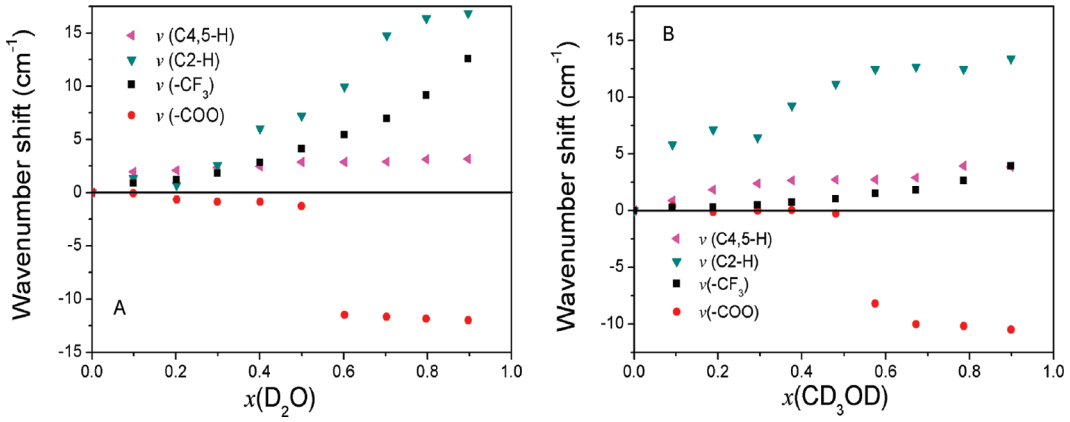

Figure 5. Wavenumber shift of C4,5−H, C2−H, $-CF_3$, and −COO stretching vibrations of two binary systems: (A) $[Bmim][CF_3CO_2]-D_2O$; (B) $[Bmim][CF_3CO_2]-CD_3OD$.

also has one functional group of OH and its methyl group can be considered as a replacement of the H atom in water. The use of deuterated methanol also aims to avoid the overlap of OH stretches and alkyl stretches in the IR spectrum.

The ATR-IR and excess infrared spectra of $[Bmim][CF_3CO_2]-CD_3OD$ mixtures at different concentrations in the region of 3200−1050 cm^{-1} are shown in Figure 4. Similar to that of the $[Bmim][CF_3CO_2]-D_2O$ system, in the ATR-IR spectra (Figure 4A, B, C), the ν(C2−H), ν(C4,5−H), ν(O−D), and $\nu(-CF_3)$ show blue shifts, while the $\nu(-COO^-)$ shows red shifts upon addition of methanol. For $\nu(-CF_3)$, only the band at 1169 cm^{-1} is focused on because the band at 1123 cm^{-1} overlaps with a band of CD_3OD. The wavenumber shifts are summarized in Figure 5B. They show a similar pattern like that of the $[Bmim][CF_3CO_2]-D_2O$ system (Figure 5A). The abrupt change in wavenumber of the $-COO^-$ group at the mole fraction of methanol of 0.5 results from the appearance of a new complex between the carbonyl group and methanol molecules as indicated in Figure 4B. The positive and negative bands in the excess infrared spectra of the $[Bmim][CF_3CO_2]-CD_3OD$ system (Figure 4D, E, F) are also similar to that of the $[Bmim][CF_3CO_2]-D_2O$ system.

In Figure 4E, the excess spectra of $\nu(-COO^-)$ show a negative band at the higher wavenumber side and a very strong positive band at the lower wavenumber side, just as in the case of Figure 3E, indicating that the H-bond involving $-COO^-$ is

dx.doi.org/10.1021/jp204305g |J. Phys. Chem. B 2011, 115, 11127–11136

enhanced with the increase of methanol concentration. Like the $[Bmim][CF_3CO_2]-D_2O$ system, we believe that methanol molecules interact mainly with the $-COO^-$ of the anion by H-bonds. For $\nu(-CF_3)$, the blue shift (Figure 4C) and the positive/negative bands in excess infrared spectra (Figure 4F) show that this group is not an inert group; most likely it contributes to the H-bonding interaction between $-COO^-$ and methanol by donating negative charges based on our previous studies.[39,63] The electron-donating effect of $-CF_3$ in the formation of methanol$\cdots[CF_3CO_2]^-$ H-bond will be confirmed by the theoretical calculation in a later section.

Compared to the $[Bmim][CF_3CO_2]-D_2O$ system, there are some interesting differences in the H-bonding interaction between $[Bmim][CF_3CO_2]$ and methanol. First, the blue shift of the stretching vibration of imidazolium ring C−H in the $[Bmim][CF_3CO_2]-CD_3OD$ system is smaller than that of the $[Bmim][CF_3CO_2]-D_2O$ system (Figure 5), indicating that the H-bond involving imidazolium ring C−H in the $[Bmim][CF_3CO_2]-CD_3OD$ system is stronger than that of the $[Bmim][CF_3CO_2]-D_2O$ system. To further compare the H-bonding interactions in the two systems, the integral values of excess molar absorbance (ε^E) for the direct interaction group $-COO^-$ have been analyzed, and the results are shown in Figure 6. The excess molar absorbances of $\nu(-COO^-)$ are both positive in the presence of D_2O and CD_3OD as shown in the figure. The excess molar absorbance of $\nu(-COO^-)$ in the $[Bmim][CF_3CO_2]-CD_3OD$ system, however, is much greater than that of the $[Bmim][CF_3CO_2]-D_2O$ system, indicating that the methanol$\cdots[CF_3CO_2]^-$ H-bond is stronger than the $H_2O\cdots[CF_3CO_2]^-$ H-bond. This strongly suggest that the methyl group of methanol has a positive contribution to the formation of the O−H$\cdots[CF_3CO_2]^-$ H-bond.

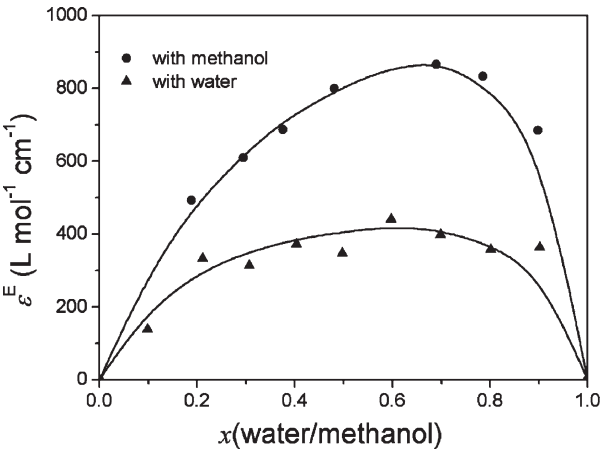

Figure 6. Integrated excess molar absorbance of −COO stretching vibrations in the binary systems of $[Bmim][CF_3CO_2]-D_2O$ and $[Bmim][CF_3CO_2]-CD_3OD$.

3.3. ^{1}H NMR Chemical Shift Analysis. ^{1}H NMR measurements of the pure IL, as well as $[Bmim][CF_3CO_2]-D_2O$ and $[Bmim][CF_3CO_2]-CD_3OD$ mixtures, were carried out at 298 K, and the chemical shift changes of individual hydrogen atoms during the dilution process were evaluated. The ^{1}H NMR chemical shift data are listed in Table SI1 in the Supporting Information.

For the $[Bmim][CF_3CO_2]-D_2O$ system, the chemical shift changes of individual hydrogen atoms are displayed in Figure 7A. The results show that the chemical shifts of C2−H, C4−H, and C5−H in the $[Bmim][CF_3CO_2]-D_2O$ system have the most significant changes and they move to high-field positions upon dilution. This indicates an increased electron density of these three acidic hydrogen atoms, a result of the weakening of the H-bonding interactions involving the C−H groups in the dialkylimidazolium ring. The chemical shifts of other hydrogen atoms in NCH_3, NCH_2, $NCCH_2$, $NCCCH_2$ and NC_3CH_3 are all slightly upfield shifted, resulting probably from the influence of H-bonding cooperativity and the solvent effect of D_2O.

For the $[Bmim][CF_3CO_2]-CD_3OD$ system, the chemical shift changes of individual hydrogen atoms are displayed in Figure 7B. Only the C2−H show an upfield shift, representative of weakening of the H-bonding interactions, and the other H atoms in C−H groups show downfield shift with the increase of methanol concentration, resulting probably from the influence of H-bonding cooperativity and the solvent effect of CD_3OD.

3.4. Quantum Chemical Calculations of the Interactions between [Bmim][CF_3CO_2] and Water/Methanol. To characterize the preferred interaction sites and to further compare the difference in the H-bonding interaction between $[Bmim][CF_3CO_2]$ and water or methanol, as many as possible orientations for each of the following complexes have been selected to perform DFT calculations: $[Bmim]^+-[CF_3CO_2]^-$, $[CF_3CO_2]^--H_2O$, $[CF_3CO_2]^-$−methanol, $[Bmim]^+-H_2O$, $[Bmim]^+$−methanol, $[Bmim][CF_3CO_2]-H_2O$, and $[Bmim][CF_3CO_2]$−methanol. The optimized geometries and corresponding interaction

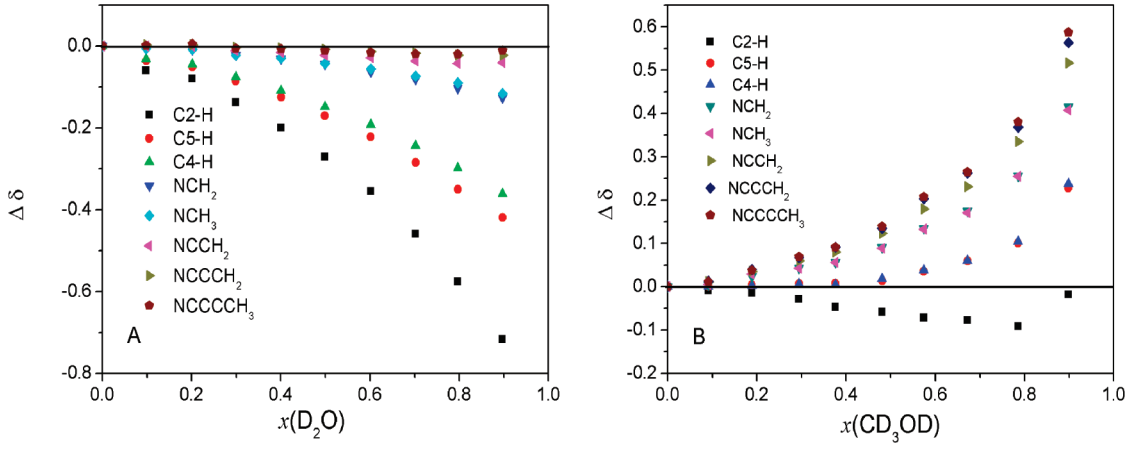

Figure 7. ^{1}H NMR chemical shift difference of the $[Bmim][CF_3CO_2]-D_2O$ system (A) and the $[Bmim][CF_3CO_2]-CD_3OD$ system (B).

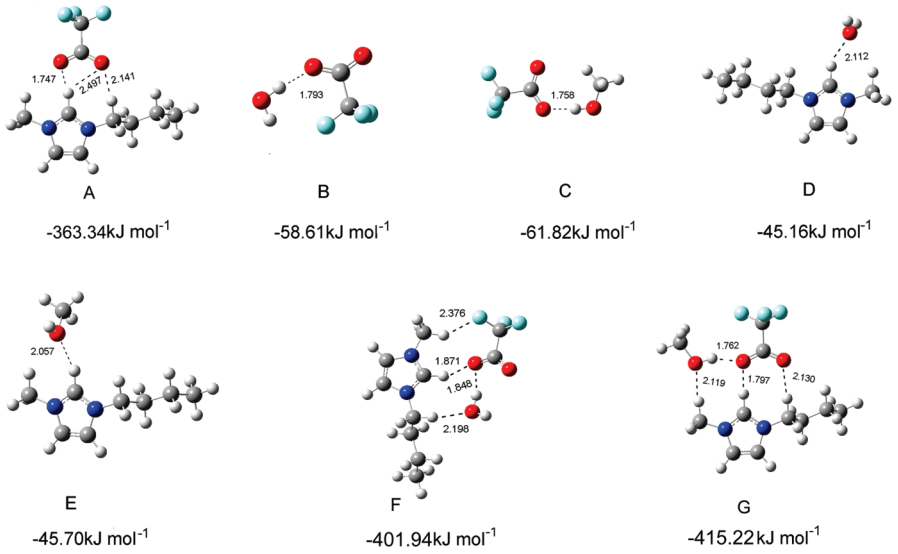

Figure 8. Optimized geometries and corresponding interaction energies of $[Bmim][CF_3CO_2]$−cosolvent systems. A, $[Bmim]^+$−$[CF_3CO_2]^-$; B, $[CF_3CO_2]^-$−H_2O; C, $[CF_3CO_2]^-$−methanol; D, $[Bmim]^+$ −H_2O; E, $[Bmim]^+$−methanol; F, $[Bmim][CF_3CO_2]$−H_2O; G, $[Bmim][CF_3CO_2]$−methanol. H-bonds are denoted by dashed lines, and the corresponding H···O or H···F distances are labeled.

energies are shown in Figure 8. The sum of van der Waals atomic radii of H and O (2.5 Å) and that of H and F atoms (2.45 Å) are used as criteria values for judging the existence of H-bonds.[76] H-bonds are denoted by dashed lines, and the corresponding H···O and H···F distances are labeled in the figure. In pure $[Bmim][CF_3CO_2]$ (Figure 8A), H-bonds can exist between the C2−H even alkyl C−H on $[Bmim]^+$ and the O═C group of the anion. In the $[CF_3CO_2]^-$−H_2O or $[CF_3CO_2]^-$−methanol complexes (Figure 8B and C), it is found that water or methanol will H-bond to $[CF_3CO_2]^-$ through their OH groups and the O═C group in $[CF_3CO_2]^-$. Namely, water or methanol interacts selectively with the O═C group but not the $-CF_3$ group in $[CF_3CO_2]^-$. In the $[Bmim]^+$−H_2O or $[Bmim]^+$−methanol complexes (Figure 8D and E), both water and methanol prefer to interact with the C2−H on $[Bmim]^+$. Comparison of the interaction pairs in Figure 8 A−E shows that all the three H-bond acceptors, $[CF_3CO_2]^-$, H_2O, and CH_3OH, can form stable H-bonds with the C2−H, consistent with the fact that the electron deficit in the imidazolium ring makes C2−H the most acidic H atom on the imidazolium ring.[6,36,51] The difference between the three acceptors is that $[CF_3CO_2]^-$ can also form H-bonds with the alkyl C−Hs on $[Bmim]^+$ at the same time. This is explained as the presence of two oxygen atoms in the carboxyl group and the resonance nature of the carboxylic group.

To understand how water or methanol interacts with both the cation and anion at the same time, we evaluated $[Bmim][CF_3CO_2]$−H_2O and $[Bmim][CF_3CO_2]$−methanol complexes. The results are depicted in Figure 8F and G. As can be seen in the figure, H-bonding interactions are present between H_2O/CH_3OH and the O atoms of $-COO^-$ group in the $[CF_3CO_2]^-$ with the O···H distances of 1.848 and 1.762 Å, respectively. H-bond is also present between $-COO^-$ group and the C2−H on the imidazolium ring with an O···H distance of 1.871 and 1.797 Å. But the O···H distances between H_2O/CH_3OH and C2−H on the imidazolium ring are 3.181 and 3.193 Å, and both are longer than the sum of van der Waals radii of H and O atoms, demonstrating that no H-bonding interaction is present between H_2O or CH_3OH and the C2−H group on the imidazolium ring at this 1:1 type of water−IL composition. This is because the interaction between the cation and anion is the strongest. Steric factors may also prevent the formation of H-bond between the cosolvent molecules with the C2−H group on the imidazolium ring. It is worth mentioning, however, that water/methanol also forms H-bonds with the alkyl C−H on $[Bmim]^+$ other than forming H-bonds with the $[CF_3CO_2]^-$, as shown in the figure.

For energetics, the interaction energy of $[Bmim]^+$−$[CF_3CO_2]^-$ (−363.34 kJ/mol) is much larger in absolute value than that of $[CF_3CO_2]^-$−H_2O (−58.61 kJ/mol) and $[Bmim]^+$−H_2O (−45.16 kJ/mol), and that of $[CF_3CO_2]^-$−methanol (−61.82 kJ/mol) and $[Bmim]^+$−methanol (−45.70 kJ/mol). The large interaction energy of $[Bmim]^+$−$[CF_3CO_2]^-$ is due to the strong electrostatic interaction of the cation and the anion. The interaction energy of $[CF_3CO_2]^-$−H_2O/methanol is larger in absolute value than that of $[Bmim]^+$−H_2O/methanol, indicating that water or methanol molecules may selectively interact with the anions at low concentrations. Furthermore, the interaction energies of $[Bmim][CF_3CO_2]$−H_2O (−401.94 kJ/mol) and $[Bmim][CF_3CO_2]$−methanol (−415.22 kJ/mol) are both larger in absolute value than that of $[Bmim]^+$−$[CF_3CO_2]^-$ (−363.34 kJ/mol). This means the mixing process of the IL and water/methanol is enthalpically favorable, a good reason for its soluble feature over the entire mole fraction range of water or methanol.

It is noteworthy that the interaction energy between methanol and $[Bmim]^+$ or $[CF_3CO_2]^-$ or $[Bmim][CF_3CO_2]$ is larger in absolute value than that in the case of H_2O, indicating that methanol interacts more strongly with the ionic species than water. Consistent with this, the H-bond distances involving methanol molecule are all shorter than those involving water molecules. All these mean that methanol is a better proton donor and proton acceptor than water when interacting with $[Bmim]^+$/$[CF_3CO_2]^-$/$[Bmim][CF_3CO_2]$. These results imply that the replacement of H in HOH by CH_3 strengthens the H-bonding interactions. Thus the methyl group is not an inert group in terms of H-bonding interactions. It plays a positive role

Table 2. Natural Population Analysis Charges (q, in e) of the $-CF_3$ Groups in $[CF_3CO_2]^-$ and Their Changes (Δq) upon Formation of $[CF_3CO_2]^-$–H_2O and $[CF_3CO_2]^-$–CH_3OH Complexes. Calculated Frequencies of the $-CF_3$ Stretching Vibrations in Each Structure Are Also Listed

			frequencies (cm^{-1})		
	$q(CF_3)$	$\Delta q(CF_3)$	ν_1	ν_2	ν_3
$[CF_3CO_2]^-$	−0.199		1129	1065	1029
$[CF_3CO_2]^-$–H_2O	−0.184	0.015	1133	1062	1046
$[CF_3CO_2]^-$–CH_3OH	−0.166	0.033	1138	1082	1044

when working as both H-bond donor and acceptor. This will be further addressed in a later section.

Similar to the CH_3 in methanol, CF_3 also act as backside group in H-bonding interactions of the studied systems. In order to understand the role of the $-CF_3$ group acting as backside group in H-bonding interactions of the studied systems, the natural population analysis (NPA) charges of the $-CF_3$ group in $[CF_3CO_2]^-$, $[CF_3CO_2]^-$–H_2O, and $[CF_3CO_2]^-$–methanol were calculated. Table 2 lists the charges (q) of the $-CF_3$ groups in the three situations and the changes of the charges (Δq) upon formation of H-bonds with H_2O and methanol. As can be seen in Table 2, the positive Δq values indicate decreases in electron density of the $-CF_3$ during the complexation. This demonstrate a electron-donating effect of the $-CF_3$ group upon the formation of H-bonds with water or methanol. Moreover, the charge change in the $[CF_3CO_2]^-$–methanol complex is greater than that in the $[CF_3CO_2]^-$–H_2O complex.

The calculated frequencies of the $-CF_3$ stretching vibrations in each structure are also listed in Table 2. Upon the formation of $[CF_3CO_2]^-$–H_2O and $[CF_3CO_2]^-$–methanol complexes, $\nu(-CF_3)$ show blue shift, consistent with the experimental results (Figure 3, Figure 4).

Finally, it is noteworthy that Figure 8 gives only some most probable geometries of the interaction complexes. They cannot represent all the possible interaction modes over the wide water and methanol concentration range. It just provides us the possible dominant interaction groups/sites between the existing species (anion, cation, and solvent molecule). At low concentration, cosolvent molecules form H-bonds with the anions. With increased water or methanol content, they will also form H-bonds with the cations. Further increasing the concentration will result in the self-associated water/methanol molecules, ion–water/methanol interaction complexes with ratios different from 1/1, and the cooperative H-bonding networks such as $[CF_3CO_2]^-$–water–water or $[CF_3CO_2]^-$–methanol–methanol complex. At high water content, cations with hydrophobic tails may also aggregate. With regard to the $[Bmim]^+$ cation examined in this work, measurements using various techniques including conductivity, surface tension, SANS, ^1H NMR, and fluorescence spectroscopy have proved that the cations could aggregate in aqueous solution like short-chain cationic surfactants with certain counterions such as $[Cl]^-$, $[BF_4]^-$, and $[C_8SO_4]^-$ locating at the outer skirt.[40−43] The critical aggregation concentration (CAC) of $[Bmim]^+$ cations depends on the nature of counterions and solvents. In the experimental systems of this work, the mole fraction of D_2O/CH_3OD increases from 0 to 1 with an increment of about 0.1. The concentration range of $[Bmim][CF_3CO_2]$ is much higher than the reported CACs of the ILs containing $[Bmim]^+$.[40−43] For example, the CAC of $[Bmim][BF_4]$ is about 1 mol kg^{-1} (about 0.018 in mole fraction) in aqueous solution.[41] Despite the difference of counterion and cosolvent between this work and the published works, it is safe to conclude that aggregated ionic clusters and ionic pairs are the dominant forms of $[Bmim][CF_3CO_2]$ in both $[Bmim][CF_3CO_2]$–D_2O and $[Bmim][CF_3CO_2]$–CD_3OD mixtures. This has been taken into account in the discussions of our infrared spectral and ^1H NMR data.

3.5. Comparison of the H-bonding Behaviors of $[Bmim][CF_3CO_2]$–Water and $[Bmim][CF_3CO_2]$–Methanol Systems: The Effect of the Back Groups. For a hydrogen-bonding interaction in the form of R–X–H···Y–R′, the back groups R and R′ are not only spectators. They play an indispensable role in the overall stability of the H-bonding interaction by charge donation/withdrawal. For the anion of the ionic liquid used in this work, as discussed above, the back group $-CF_3$ bonded to the proton acceptor $-COO^-$ has a electron-donating effect on the H-bonding interaction between $-COO^-$ and water or methanol, leading to blue shift of $\nu(-CF_3)$.

For the cosolvent methanol, the methyl group plays also an important role in the H-bonding interaction. Comparing methanol and the other cosolvent water, it was found that, with the increase of concentration of cosolvents, the H-bond involving imidazolium ring C–H in the $[Bmim][CF_3CO_2]$–CD_3OD system is stronger than that of the $[Bmim][CF_3CO_2]$–D_2O system, and the excess molar absorbance of $\nu(-COO^-)$ in the $[Bmim][CF_3CO_2]$–CD_3OD system is much greater than that of the $[Bmim][CF_3CO_2]$–D_2O system. These spectroscopic and quantum chemical results suggest that methanol is a better proton donor/proton acceptor than water when interacting with $[Bmim]^+/[CF_3CO_2]^-/[Bmim][CF_3CO_2]$. Namely, the methyl group in methanol has a positive contribution to the formation of O–H···$[CF_3CO_2]^-$ and O···$[Bmim]^+$ H-bonds.

For the system of pyridinium-based IL $[Bpy][BF_4]$ + DMSO we reported recently,[39] the back alkyl groups in both pyridinium ring and DMSO exhibit positive influence on the H-boding interaction. It was found that the butyl group in the cation is an electron acceptor, while the methyl groups in DMSO are electron donors.

The above discussion strongly suggests that methanol is a very good model molecule in studying the hydrogen-bonding interactions. We have demonstrated this in a study of DMSO–methanol interactions.[63] This is also in line with the viewpoint of a recent work, which pointed out that the chemical structure of methanol offers an opportunity to explore the effects of both proper and improper hydrogen bonding.[77]

4. CONCLUSIONS

In this work, the H-bonding interactions in two binary mixtures, $[Bmim][CF_3CO_2]$–water and $[Bmim][CF_3CO_2]$–methanol, have been studied by a combined application of FTIR spectroscopy, NMR, and DFT calculations. It is found that water or methanol, at limiting concentrations, interacts preferentially with the $-COO^-$ group in the ionic liquid $[Bmim][CF_3CO_2]$. The $-CF_3$ group has a electron-donating effect to strengthen the H-bonding interaction between $-COO^-$ and water or methanol. In comparison of the two protonic solvents, water and methanol, it was found that the methanol···$[CF_3CO_2]^-/[Bmim]^+$ H-bond is stronger than the H_2O···$[CF_3CO_2]^-/[Bmim]^+$ H-bond. This means that the methyl group has a positive

contribution on the formation of O−H···$[CF_3CO_2]^-$ and O···$[Bmim]^+$ H-bond. In comparison of the pair-interaction energetics among the species $[Bmim]^+$, $[CF_3CO_2]^-$, water, and methanol, the following sequential order of interaction strength is obtained: $[Bmim]^+$−methanol−$[CF_3CO_2]^-$ > $[Bmim]^+$−water−$[CF_3CO_2]^-$ > $[Bmim]^+$ − $[CF_3CO_2]^-$ > $[CF_3CO_2]^-$−methanol > $[CF_3CO_2]^-$−water > $[Bmim]^+$−methanol > $[Bmim]^+$−water. These studies on H-bonding interactions between [Bmim]$[CF_3CO_2]$ and water/methanol deepened our understanding of the physical properties of the hydrophilic Brønsted acidic ILs and their mixtures with protonic-type solvents.

■ ASSOCIATED CONTENT

Supporting Information. ^{1}H NMR chemical shift data (Table SI1). This material is available free of charge via the Internet at http://pubs.acs.org.

■ AUTHOR INFORMATION

Corresponding Author
*Phone (+86) 10 6279 2492; fax (+86) 10 6277 1149; e-mail yuzhw@tsinghua.edu.cn.

■ ACKNOWLEDGMENT

This work was supported by the Natural Science Foundation of China (Project No. 20973100 and 21003081).

■ REFERENCES

(1) *Ionic Liquids Industrial Applications for Green Chemistry*; Rogers, R. D., Seddon, K. R., Eds.; ACS Symposium Series 818; American Chemical Society: Washington, DC, 2002.
(2) *Ionic Liquids as Green Solvent*; Rogers, R. D., Seddon, K. R., Eds.; ACS Symposium Series 856; American Chemical Society: Washington, DC, 2003; Chapter 12.
(3) *Ionic Liquids IIIA: Fundamentals, Progress, Challenges, and Opportunities: Properties and Structure*; Rogers, R. D., Seddon, K. R., Eds.;American Chemical Society: Washington, DC, 2005; Vol. 901.
(4) Earle, M.; Forestier, A.; Olivier-Bourbigou, H.; Wasserscheid, P. *Ionic Liquids in Synthesis*; Wasserscheid, P., Welton, T., Eds.; Wiley−VCH Verlag: Weinheim, Germany, 2003.
(5) Welton, T. *Chem. Rev.* **1999**, *99*, 2071–2083.
(6) Fumino, K.; Wulf, A.; Ludwig, R. *Angew. Chem., Int. Ed.* **2008**, *47*, 8731–8734.
(7) Dupont, J.; de Souza, R. F.; Suarez, P. A. Z. *Chem. Rev.* **2002**, *102*, 3667–3692.
(8) Macfarlane, D. R.; Seddon, K. R. *Aust. J. Chem.* **2007**, *60*, 3–5.
(9) Zhao, H.; Xia, S.; Ma, P. *J. Chem. Technol. Biotechnol.* **2005**, *80*, 1089–1096.
(10) Krossing, I.; Slattery, J. M. *Z. Phys. Chem.* **2006**, *220*, 1343–1359.
(11) Holbrey, J. D.; Reichert, W. M.; Swatloski, R. P.; Seddon, K. R.; Rogers, R. D. *Green Chem.* **2002**, *4*, 407–413.
(12) Borra, E. F.; Seddiki, O.; Angel, R.; Eisenstein, D.; Hickson, P.; Seddon, K. R.; Worden, S. P. *Nature* **2007**, *447*, 979–981.
(13) Torrecilla, J. S.; Rojo, E.; García, J.; Rodríguez, F. *Ind. Eng. Chem. Res.* **2008**, *47*, 4025–4028.
(14) Ficke, L. E.; Rodríguez, H.; Brennecke, J. F. *J. Chem. Eng. Data* **2008**, *53*, 2112–2119.
(15) González, E. J.; González, B.; Calvar, N.; Domínguez, A. *J. Chem. Eng. Data* **2007**, *52*, 1641–1648.
(16) Torrecilla, J. S.; Rafione, T.; García, J.; Rodríguez, F. *J. Chem. Eng. Data* **2008**, *53*, 923–928.
(17) Fröba, A. P.; Wasserscheid, P.; Gerhard, D.; Kremer, H.; Leipertz, A. *J. Phys. Chem. B* **2007**, *111*, 12817–12822.
(18) Rogers, R. D.; Seddon, K. R. *Science* **2003**, *302*, 792–793.
(19) Carvalho, P. J.; Alvarez, V. H.; Schroeder, B.; Gil, A. M.; Marrucho, I. M.; Aznar, M.; Santos, L. M. N. B. F.; Coutinho, J. A. P. *J. Phys. Chem. B* **2009**, *113*, 6803–6812.
(20) Plechkova, N. V.; Seddon, K. R. *Chem. Soc. Rev.* **2008**, *37*, 123–150.
(21) Ficke, L. E.; Brennecke, J. F. *J. Phys. Chem. B* **2010**, *114* (32), 10496–10501.
(22) Seddon, K. R.; Stark, A.; Torres, M. J. *Pure Appl. Chem.* **2000**, *72*, 2275–2287.
(23) Huddleston, J. G.; Visser, A. E.; Reichert, W. M.; Willauer, H. D.; Broker, G. A.; Rogers, R. D. *Green Chem.* **2001**, *3*, 156–164.
(24) Marsh, K. N.; Boxall, J. A.; Lichtenthaler, R. *Fluid Phase Equilib.* **2004**, *219*, 93–98.
(25) Mayrand-Provencher, L.; Rochefort, D. *J. Phys. Chem. C* **2009**, *113*, 1632–1639.
(26) Le Bideau, J.; Viaub, L.; Vioux, A. *Chem. Soc. Rev.* **2011**, *40*, 907–925.
(27) Wang, Y.; Radosevich, M.; Hayes, D.; Labbe, N. *Biotechnol. Bioeng.* **2011**, *108*, 1042–1048.
(28) Arbizzani, C.; Gabrielli, G.; Mastragostino, M. *J. Power Sources* **2011**, *196*, 4801–4805.
(29) Zhang, X. Y.; Li, D. F.; Jia, X. F.; Wang, J. J.; Fan, X. S. *Catal. Commun.* **2011**, *12*, 839–843.
(30) Fang, D.; Yang, J. M.; Liu, Z. L. *J. Heterocycl. Chem.* **2011**, *48*, 468–472.
(31) Kelkar, M. S.; Shi, W.; Maginn, E. J. *Ind. Eng. Chem. Res.* **2008**, *47*, 9115–9126.
(32) Wang, J. F.; Li, C. X.; Wang, Z. H. *J. Chem. Eng. Data* **2007**, *52*, 1307–1312.
(33) Widegren, J. A.; Saurer, E. M.; Marsh, K. N.; Magee, J. W. *J. Chem. Thermodyn.* **2005**, *37*, 569–575.
(34) Heintz, A.; Lehmann, J. K.; Wertz, C.; Jacquemin, J. *J. Chem. Eng. Data* **2005**, *50*, 956–960.
(35) Najdanovic-Visak, V.; Rebelo, L. P. N.; Ponte, da M. N. *Green Chem.* **2005**, *7*, 443–450.
(36) Zhang, L. Q.; Wang, Y.; Xu, Z.; Li, H. R. *J. Phys. Chem. B* **2009**, *113*, 5978–5984.
(37) Zhang, L. Q.; Xu, Z.; Wang, Y.; Li, H. R. *J. Phys. Chem. B* **2008**, *112*, 6411–6419.
(38) Zhang, Q. G.; Wang, N. N.; Yu, Z. W. *J. Phys. Chem. B* **2010**, *114*, 4747–4754.
(39) Wang, N. N.; Zhang, Q. G.; Wu, F. G.; Li, Q. Z.; Yu, Z. W. *J. Phys. Chem. B* **2010**, *114*, 8689–8700.
(40) Zhao, Y.; Gao, S. J.; Wang, J. J.; Tang, J. M. *J. Phys. Chem. B* **2008**, *112*, 2031–2039.
(41) Wang, J. J.; Wang, H. Y.; Zhang, S. L.; Zhang, H. C.; Zhao, Y. *J. Phys. Chem. B* **2007**, *111*, 6181–6188.
(42) Singh, T.; Kumar, A. *J. Phys. Chem. B* **2007**, *111*, 7843–7851.
(43) Bowers, J.; Butts, C. P.; Martin, P. J.; Vergara-Gutierrez, M. C.; Heenan, R. K. *Langmuir* **2004**, *20*, 2191–2198.
(44) Köddermann, T.; Wertz, C.; Heintz, A.; Ludwig, R. *Angew. Chem., Int. Ed.* **2006**, *45*, 3697–3702.
(45) Cammarata, L.; Kazarian, S. G.; Salterb, P. A.; Welton, T. *Phys. Chem. Chem. Phys.* **2001**, *3*, 5192–5200.
(46) Porter, A. R.; Liem, S. Y.; Popelier, P. L.A. *Phys. Chem. Chem. Phys.* **2008**, *10*, 4240–4248.
(47) Katayanagi, H.; Nishikawa, K.; Shimozaki, H.; Miki, K.; Westh, P.; Koga, Y. *J. Phys. Chem. B* **2004**, *108*, 19451–19457.
(48) Miki, K.; Westh, P.; Nishikawa, K.; Koga, Y. *J. Phys. Chem. B* **2005**, *109*, 9014–9019.
(49) Takamuku, T.; Kyoshoin, Y.; Shimomura, T.; Kittaka, S.; Yamaguchi, T. *J. Phys. Chem. B* **2009**, *113*, 10817–10824.
(50) Chang, H. C.; Jiang, J. C.; Tsai, W. C.; Chen, G. C.; Lin, S. H. *J. Phys. Chem. B* **2006**, *110*, 3302–3307.
(51) Köeddermann, T.; Wertz, C.; Heintz, A.; Ludwig, R. *ChemPhysChem* **2006**, *7*, 1944–1949.
(52) Köddermann, T.; Paschek, D.; Ludwig, R. *ChemPhysChem* **2008**, *9*, 549–555.

(53) Jeon, Y.; Sung, J.; Kim, D.; Seo, C.; Cheong, H.; Ouchi, Y.; Ozawa, R.; Hamaguchi, H. *J. Phys. Chem. B* **2008**, *112*, 923–928.
(54) Moreno, M.; Castiglione, F.; Mele, A.; Pasqui, C.; Raos, G. *J. Phys. Chem. B* **2008**, *112*, 7826–7836.
(55) Lasségues, J. C.; Grondin, J.; Cavagnat, D.; Johansson, P. *J. Phys. Chem. A* **2009**, *113*, 6419–6421.
(56) Carvalho, P. J.; Alvarez, V. H.; Schroeder, B.; Gil, A. M.; Marrucho, I. M.; Aznar, M.; Santos, L. M. N. B. F.; Coutinho, J. A. P. *J. Phys. Chem. B* **2009**, *113*, 6803–6812.
(57) Shiflett, M. B.; Yokozeki, A. *J. Chem. Eng. Data* **2009**, *54*, 108–114.
(58) Bonhote, P.; Dias, A. P.; Papageorgiou, N.; Kalyanasundaram, K.; Gratzel, M. *Inorg. Chem.* **1996**, *35*, 1168–1178.
(59) Wu, F. G.; Wang, N. N.; Yu, J. S.; Luo, J. J.; Yu, Z. W. *J. Phys. Chem. B* **2010**, *114*, 2158–2164.
(60) Wang, N. N.; Jia, Q.; Li, Q. Z.; Yu, Z. W. *J. Mol. Struct.* **2008**, *883−884*, 55–60.
(61) Wang, N. N.; Li, Q. Z.; Yu, Z. W. *Appl. Spectrosc.* **2009**, *63*, 1356–1362.
(62) Li, Q. Z.; Wang, N. N.; Zhou, Q.; Sun, S. Q.; Yu, Z. W. *Appl. Spectrosc.* **2008**, *62*, 166–170.
(63) Li, Q. Z.; Wu, G. S.; Yu, Z. W. *J. Am. Chem. Soc.* **2006**, *128*, 1438–1439.
(64) Koga, Y.; Sebe, F.; Minami, T.; Otake, K.; Saitow, K.; Nishikawa, K. *J. Phys. Chem. B* **2009**, *113*, 11928–11935.
(65) Suarez, P. A. Z.; Consorti, C. S.; de Souza, R. F.; Dupont, J.; Goncalves, R. S. *J. Braz. Chem. Soc.* **2002**, *13*, 106–109.
(66) Hansen, W. N. *Spectrochim. Acta* **1965**, *21*, 815–833.
(67) Frisch, M. J.; Trucks, G. W.; Schlegel, H. B.; Scuseria, G. E.; Robb, M. A.; Cheesman, J. R.; Zakrzewski, V. G.; Montgomery, J. A., Jr.; Stratmann, R. E.; Burant, J. C.; Dapprich, S.; Millam, J. M.; Daniels, A. D.; Kudin, K. N.; Strain, M. C.; Farkas, O.; Tomasi, J.; Barone, V.; Cossi, M.; Cammi, R.; Mennucci, B.; Pomelli, C.; Adamo, C.; Clifford, S.; Ochterski, J.; Petersson, G. A.; Ayala, P. Y.; Cui, Q.; Morokuma, K.; Malick, D. K.; Rabuck, A. D.; Raghavachari, K.; Foresman, J. B.; Cioslowski, J.; Ortiz, J. V.; Baboul, A. G.; Stefanov, B. B.; Liu, G.; Liashenko, A.; Piskorz, P.; Komaromi, I.; Gomperts, R; Martin, R. L.; Fox, D. J.; Keith, T.; Al-Laham, M. A.; Peng, C. Y.; Nanayakkara, A.; Gonzalez, C.; Challacombe, M.; Gill, P. M. W.; Johnson, B.; Chen, W.; Wong, M. W.; Andres, J. L.; Gonzalez, C.; Head-Gordon, M.; Replogle, E. S.; Pople, J. A. *Gaussian 03*, revision B.03; Gaussian Inc.: Pittsburgh, PA, 2003.
(68) Dhumal, N. R.; Kim, H. J.; Kiefer, J. *J. Phys. Chem. A* **2009**, *113*, 10397–10404.
(69) Talaty, E. R.; Raja, S.; Storhaug, V. J.; Dolle, A.; Carper, W. R. *J. Phys. Chem. B* **2004**, *108*, 13177–13184.
(70) Izgorodina, E. I.; Bernard, U. L.; MacFarlane, D. R. *J. Phys. Chem. A* **2009**, *113*, 7064–7072.
(71) Socrates, G. *Infrared Characteristic Group Frequencies*; John Wiley & Sons: Chichester, U.K., 1980; pp 91−92.
(72) Kiefer, J.; Fries, J.; Leipertz, A. *Appl. Spectrosc.* **2007**, *61*, 1306–1311.
(73) Joseph, J.; Jemmis, E. D. *J. Am. Chem. Soc.* **2007**, *129*, 4620–4632.
(74) Fawcett, W. R.; Kloss, A. A. *J. Phys. Chem. B* **1996**, *100* 2019–2024.
(75) Abraham, M. H.; Platts, J. A. *J. Org. Chem.* **2001**, *66*, 3484–3491.
(76) Pauling, L. *The Nature of the Chemical Bond*, 3rd ed.; Cornell University Press: New York, 1960.
(77) Keefe, C. D.; Istvankova, Z. *Can. J. Chem.* **2011**, *89*, 34–46.